Synthesis of geochemical techniques to identify the origin and multistage evolution of saline water in a complex geothermal system

Yinlei Hao[1,2,3], *Zhonghe* Pang[1,2,3,*], *Tianming* Huang[1,2,3], *Yanlong* Kong[1,2,3], *Jiao* Tian[1,2,3], and *Yingchun* Wang[1,2,3]

[1]Key Laboratory of Shale Gas and Geoengineering, Institute of Geology and Geophysics, Chinese Academy of Sciences, 100029, Beijing, China
[2]Institute of Earth Sciences, Chinese Academy of Sciences, 100029, Beijing, China
[3]University of Chinese Academy of Sciences, 100049, Beijing, China

Abstract. Elucidating brine origin and evolution is a fundamental but not easy task especially for coastal geothermal systems with possible marine constituents and multistage evolution, as subsequently physical, chemical and biological alteration processes may mask the original and early-stage signatures. Here chemical and isotopic characteristics of water (D and ^{18}O) and dissolved constituents (^{13}C, ^{14}C, ^{11}B and $^{87}Sr/^{86}Sr$) have been utilized to investigate the source and multistage evolution of the Jimo coastal geothermal system in eastern China, with dramatic differences of geochemical characteristics observed within a 0.2 km^2 area. Results show that geothermal water is derived from paleo-meteoric water and has undergone a 3-stages evolution that involves: (1) Dissolution of marine halite and potash salts in the deep reservoir; (2) Water-rock reactions especially cation exchange produces a Cl-Na-Ca type water as deep geothermal water upwells along the fault zone; (3) A minor (<0.3%) addition of fossil seawater to the shallow aquifer that produces Cl-Na type waters in the west, whereas sulfide oxidation and dissolution of aluminosilicate and carbonates in the east produces Cl-Na-Ca type waters. The methodology utilized in this study offers a means of examining other similar complex geochemical systems having a multistage evolution.

1 Introduction

A clear understanding of brine origin and evolution in coastal geothermal systems is necessary for the sustainable management of geothermal waters. Although numerous chemical and isotopic techniques have been developed, exclusive identification the salinity of coastal geothermal waters with marine or non-marine origin is still difficult like some modern non-marine saline lakes exhibit similar chemical compositions to evaporated water [1, 2]. Research about detailed delineation of geothermal waters evolution pattern at different stage is relatively scarce, which may be contributed to that subsequently

* Corresponding author: z.pang@mail.iggcas.ac.cn

complicated physical (mixing with shallow groundwater), chemical (dolomitization, ion exchange) and biological (sulfate reduction) processes can generally cover up the early stage signals along the flow path [3]. This paper investigates the multistage evolution of Jimo coastal geothermal system with dramatic differences of geochemical characteristics within a 0.2 km^2 area to discern the origin and evolution of geothermal both water and dissolved constituents.

2 Geological setting

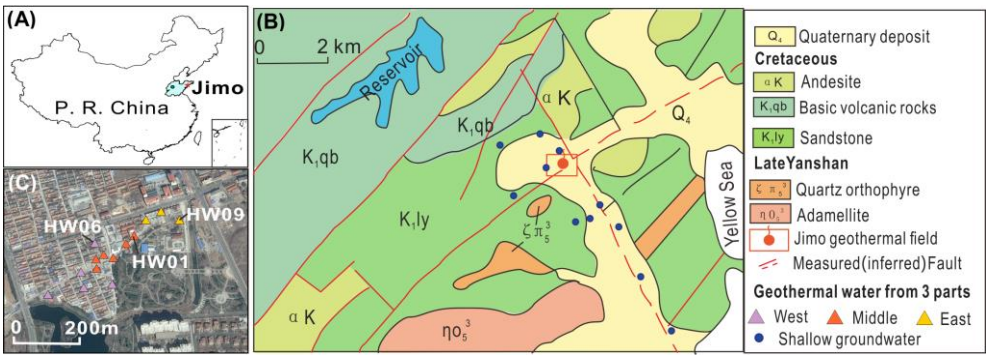

Fig. 1. (A) The geographical location of study area; (B) The geological sketch map of study area; and sampling sites; (C) Sampling locations of geothermal water.

Study area is located in the southeastern Jiaodong Peninsula of China, neighbouring Yellow Sea (Fig. 1A). Tectonically, this area belongs to Muping-Jimo fault zone, an important part of giant Tanlu strike-slip fault system in the eastern China. The structure in the study area is mainly controlled by NE and NW trending faults. Early Cretaceous Laiyangqun clastic rocks and Qingshan pyroclastic rocks composed of sandstone, conglomerate, mudstone and intermediate-acid and intermediate-basic volcanics are widely distributed (Fig. 1B). The depth of Quaternary unconsolidated sediments in the geothermal field is 10-25 m. From bottom to top, the types of sediments are Holocene black marine mud, brown lagoon clay and lacustrine silty sediment. X-ray diffraction analysis has identified salt, gypsum and natural sulfur in the hydrothermal and silicious sediments of the study area [4].

3 Hydrochemical characteristics

The locations of sampling sites in the study area are shown in Figure 1 (B, C). And three distinct parts (west, middle and east) have been identified based on geographic location, temperatures, TDS, pH and ORP of geothermal water. Most geothermal waters are Cl-Na-Ca type, except for three samples from west area are Cl-Na type. Temperature decreases from 80-89.5°C in the middle of the study area to 49.2-70.2°C in the west and 60-66.9°C in the east. Total dissolved solids (TDS) ranges from 2.47 to 10.83 g/L and exhibits a similar trend to temperature. TDS and temperature from HW01 well are highest, which is consistent with the results of geophysical survey that the upward channel of deep saline water is nearest to the location of HW01 well. However, pH tends to increase from 4.19 in the east to 7.48 in the west. Oxidation reduction potential (ORP) values decrease from 157 mV in the east to -45 mV in the west, indicating that an acid-oxidizing environment in the east gradually transitions into a weakly alkaline-reducing environment in the west.

4 Origin and evolution of geothermal water

4.1 The origin of geothermal water

Geothermal water and shallow groundwater in the study area lying on the local meteoric water line (LMWL) indicate the dominated meteoric origin (Fig. 2A). The relative depleted isotopic composition of geothermal waters and 14C age of 10,010 B.P. reflect that geothermal water is recharged during Pleistocene glacial period with a cooler climate. $\delta^{18}O$ values increase with Cl concentration decrease reflect mixing of shallow groundwater recharged by meteoric water rather than seawater as geothermal water flows from middle to west and east (Fig. 2B).

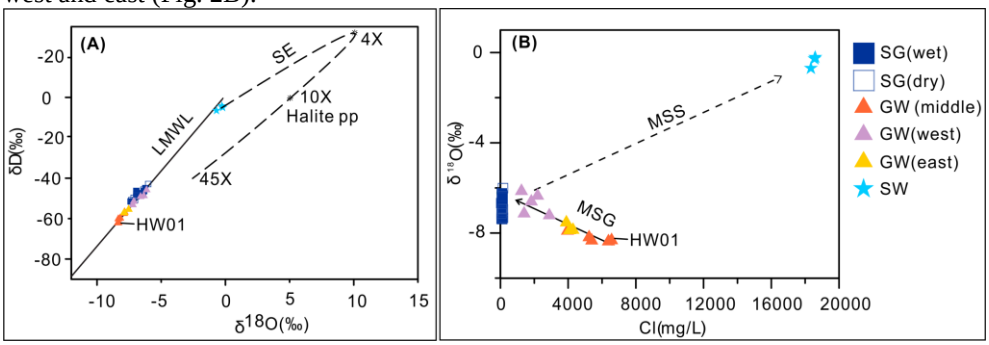

Fig. 2. (A) Plot of δD versus $\delta^{18}O$ for waters in the Jimo basin; Legend: Shallow groundwater (SG), Geothermal water (GW), Seawater (SW), Local Meteoric Water Line (LMWL), Halite precipitation (Halite pp), Seawater Evaporation line (SE) [5]; (B) Plot of $\delta^{18}O$ versus Cl showing possible mixing trends: MSG: mixing of shallow groundwater, MSS: mixing of shallow groundwater and seawater.

4.2 Stage 1: Dissolved marine salts

Geothermal waters in the middle area with least secondary modifications are characterized by Na/Cl and Br/Cl molar ratio of 0.63 to 0.69 and 0.00079 to 0.0010, respectively, both lower than seawater, which is quite different from characteristics of typical geothermal systems with a non-marine, seawater or fossil seawater origin in eastern coastal area of China [1]. A Br/Cl-Na/Cl ratio plot has been established to identify the different origin of salinity like non-marine, seawater, fossil seawater and evaporites dissolution. The advantage of using this diagram is insensitivity to dilution by freshwater. As Fig. 3A shows, synchronous dissolution of marine halite and potash salts from the final stages of seawater evaporation (e.g., sylvite) is most likely to be source of deep geothermal water, which is further verified by B isotopic signatures. The $\delta^{11}B$ values of geothermal water in the middle area ranges from 15.9 to 17.23 ‰, which is comparable to the isotopic compositions of marine salts [7].

4.3 Stage 2: Water-rock reactions in the sandstone

The $^{87}Sr/^{86}Sr$ ratios of geothermal water (0.709233 to 0.710726) are close to the bulk host sandstone (0.710433) indicating that Sr results from water and sandstone reaction. Calcium and magnesium content variation also provides specific information of water-rock interaction. Geothermal water samples are placed above the carbonates and sulfates dissolution line with a slope of 1:1, especially for geothermal water in the middle area with $(Ca^{2+}+Mg^{2+})/ (HCO_3^-+SO_4^{2-})$ ratios from 9 to 19 (Fig. 4A), illustrating the dissolution of

carbonates and sulfates are not the main source of Ca^{2+} and Mg^{2+} and other processes such as cation exchange or dissolution of other calcium and magnesium minerals. Cation exchange has been supported by Chloro-alkaline CAI 1 and CAI 2 [8]. Fig. 4B shows the scatter plot of CAI 1 against CAI 2, in which all geothermal water samples exhibit positive values for both indices, indicating that cation exchange of Na^+ and K^+ in the water substitute for Ca^{2+} and Mg^{2+} in the rock. And the indices of HW01 are highest with values of 0.34 for CAI 1 and 16.7 for CAI 2, suggesting that cation exchange process significant elevates Ca and Mg content as deep hot geothermal water upwells along the fault zone. During this period, saline waters changed into a Cl-Na-Ca water type. Shallow secondary processes have made pattern of (Ca^{2+}+Mg^{2+}) versus (HCO_3^-+SO_4^{2-}) evolve in two direction (Fig. 4A), which will discuss later.

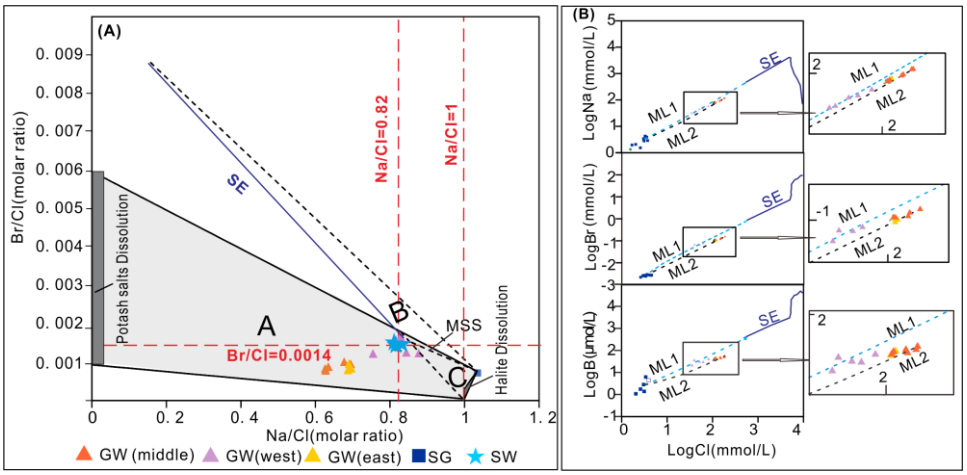

Fig. 3. (A) Br/Cl-Na/Cl molar ratio diagram for waters from the Jimo basin illustrating the possible different origins of salinity: A - Mixture of waters derived from halite dissolution and the dissolution of potash salts; B - Mixing of evaporated seawater and shallow groundwater; C - mixing of a halite-derived solution and seawater; B+C - Mixture of halite-derived solution and evaporated seawater. The Br/Cl and Na/Cl molar ratio of water modified by mixing and addition of solid solutes is calculated based on the method given by [6]. (B) Log-scale plots of Na versus Cl, Br versus Cl, and B versus Cl for waters in the Jimo basin showing the mixing trends for the mixing trend of seawater and shallow groundwater (ML1), and the mixing of HW01 and shallow groundwater (ML2).

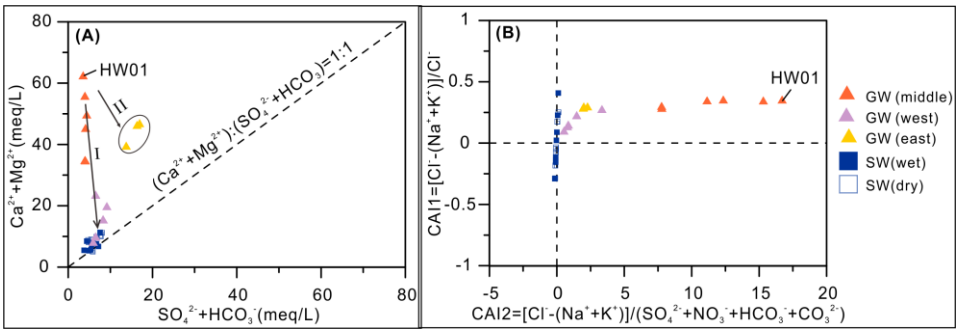

Fig. 4. Plots of (A) Ca^{2+}+Mg^{2+} versus HCO_3^-+SO_4^{2-}, expressed as meq/L showing the evolution of geothermal water in two directions dominantly influenced by the mixing with shallow groundwater (I) and for sulfide oxidation and carbonates dissolution (II) and (B) CAI 1 versus CAI 2 for waters in the Jimo basin.

4.4 Stage 3: Shallow secondary modified processes

When geothermal water flows from the middle of the geothermal area to the west and east areas, shallow secondary processes act to produce a Cl-Na water type in the west area. Geothermal water gradually approaches seawater in composition in the west area (Fig. 3A), and the shallow groundwater mixing line of Na versus Cl, Br versus Cl, B versus Cl (Fig. 3B) is consistent with the signature of addition of fossil seawater trapped in the sediments, especially for HW06 with higher Br/Cl and I/Cl molar ratios than seawater. Based on $\delta^{11}B$ values and B/Cl ratios, the proportion of extracted fossil seawater is quite small (less than 0.3%). The acid-oxidizing environment with pH of 4.19 and ORP of 157 mV, high SO_4 concentration, SO_4/Cl molar ratio and significant increase of Fe/Cl, Al/Cl, Ca/Cl, Mg/Cl and Sr/Cl ratios shown in in the east area indicate sulfide oxidation dominated by pyrite, aluminosilicate and carbonates dissolution are the predominant geochemical processes, which are consistent with the pattern II of the elevated (Ca^{2+}+Mg^{2+}) and (HCO_3^-+SO_4^{2-}) in contrast with the pattern I dominantly influenced by mixing of shallow groundwater (Fig. 4A). Besides, negative saturation indexes (SI < 0) reveals that kaolinite, microcline, Ca-montmorillonite and Mg-montmorillonite, calcite, dolomite, and strontianite are undersaturated in the east area, which is different with equilibrium and oversaturated state in the west and middle area.

5 Conclusions

The Jimo geothermal system is recharged by paleo-meteoric water and has undergone dissolution marine halite and potash salts, cation exchange, addition of fossil seawater and sulfide oxidation.

This work was supported by the National Natural Science Foundation of China (NSFC Grant 41430319).

References

1. L. Chen, et al., *J Volcan Geotherm, Res* **318**, 45-54 (2016)
2. A. Vengosh, et al., *Appl Geochem*, **17**, 163-183 (2002)
3. J. Mahlknecht, et al., *Sci Total Environ*, **587–588**, 282-295 (2017)
4. G. Luan, et al., *Acta Geoscientica Sinica*, **28**, 418-427 (2007)
5. L.P. Knauth, et al., Geochim Cosmochim Acta, **50**, 419-433 (1986)
6. F.J. Alcalá, et al., *Hydrogeol J*, **359**, 189-207 (2008)
7. A. Vengosh, et al, *Geology*, **20**, 799-802 (1992)
8. H. Scholler, *Water Res*, **33,** 44-52 (1967)